Article

Molecular Basis of DNA Photodimerization: Intrinsic Production of Cyclobutane Cytosine Dimers

Daniel Roca-Sanjua#n, Gloria Olaso-Gonza#lez, Israel Gonza#lez-Rami#rez, Luis Serrano-Andre#s, and Manuela Mercha#n

J. Am. Chem. Soc., **2008**, 130 (32), 10768-10779 • DOI: 10.1021/ja803068n • Publication Date (Web): 16 July 2008

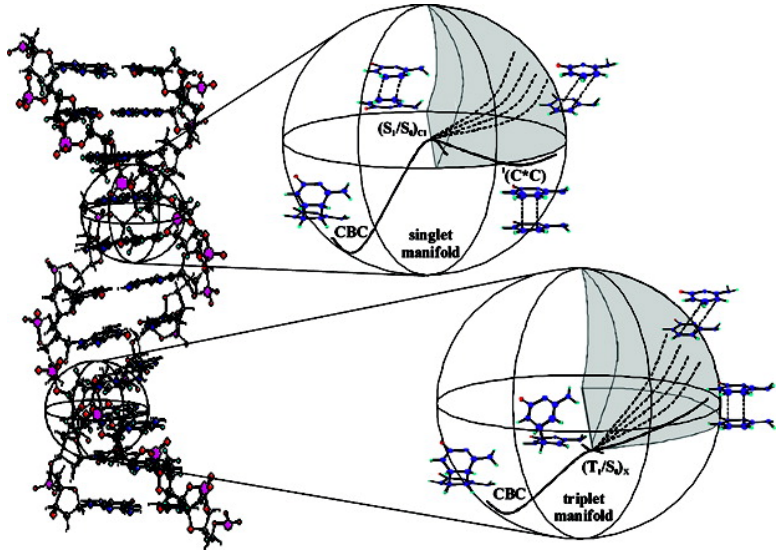

More About This Article

Additional resources and features associated with this article are available within the HTML version:

- Supporting Information
- Links to the 3 articles that cite this article, as of the time of this article download
- Access to high resolution figures
- Links to articles and content related to this article
- Copyright permission to reproduce figures and/or text from this article

View the Full Text HTML

J|A|C|S
ARTICLES

Published on Web 07/16/2008

Molecular Basis of DNA Photodimerization: Intrinsic Production of Cyclobutane Cytosine Dimers

Daniel Roca-Sanjuán, Gloria Olaso-González, Israel González-Ramírez, Luis Serrano-Andrés, and Manuela Merchán*

Instituto de Ciencia Molecular, Universitat de València, Apartado 22085, ES-46071 Valencia, Spain

Received April 25, 2008; E-mail: Manuela.Merchan@uv.es

Abstract: Based on CASPT2 results, the present contribution establishes for the first time that cytosine photodimer formation (C<>C) is mediated along the triplet and singlet manifold by a singlet−triplet crossing, $(T_1/S_0)_X$, and by a conical intersection, $(S_1/S_0)_{CI}$, respectively. The former can be accessed in a barrierless way from a great variety of photochemical avenues and exhibits a covalent single bond between the ethene $C_6-C_{6'}$ carbon atoms of each monomer. The efficiency of the stepwise triplet mechanism, however, would be modulated by the effectiveness of the intersystem crossing mechanism. The results provide the grounds for the understanding of the potential photogenotoxicity of endogenous and exogenous compounds via triplet−triplet sensitization, with a lower bound for cytosine oligonucleotides predicted to be 2.70 eV, and give support to the traditional view of the primary role of triplet excited states in the photochemistry of DNA, a well-known source of photoproducts in solution under triplet photosensitization conditions. The function played by singlet excimers (excited dimers) to explain both the red-shifted fluorescence and photoreaction is highlighted. A rationale on the pronounced wavelength dependence of the observed fluorescence is offered. Geometrical arrangements at the time of light irradiation close to, but energetically above, $(S_1/S_0)_{CI}$ are suggested as *reactive orientations* that become prone to produce C<>C directly, with no energy barrier. Because of the outstanding intrinsic ability of cytosine to form stable relaxed excimers, the system located near the bound relaxed excimer has to accumulate enough vibrational energy to surmount a small barrier of 0.2 eV to reach $(S_1/S_0)_{CI}$, making the overall process to proceed at a slower relative rate as compared to other compounds such as thymine, which is not susceptible of forming so stable excimers.

Introduction

Cyclobutane pyrimidine dimers (Pyr<>Pyr) formed by adjacent pyrimidine bases can be considered the most frequent lesion induced in ultraviolet (UV)-irradiated *cellular* DNA, occurring with a yield of formation 1 order of magnitude larger than pyrimidine 6-4 pyrimidone photoproducts.[1,2] Living organisms are able to reverse the photodamage by using DNA photolyase enzymatic repair, which catalyzes the cleavage of the $C_5-C_{5'}$ and $C_6-C_{6'}$ bonds of the formed Pyr<>Pyr, restoring the pyrimidines to their native state. The different DNA repair enzymes usually involve electron transfer from a catalytic cofactor to the dimer.[3] The Pyr<>Pyr photoproducts are lesions normally associated with various lethal biological responses happening at the cellular level since they inhibit DNA replication and transcription.[1,4,5] The different mechanisms proposed for Pyr<>Pyr production[1] involve singlet and triplet states of the monomers in solution and singlet states of vertical stacked nucleobases in the solid state, respectively. The efficiency of the photodimerization markedly depends on the experimental conditions (solvent, aggregation state, pH, degree of hydratation), the sequence of nucleotides, and the type (A-, B-like) of DNA conformation. It is also worth mentioning the vast amount of literature where the presence of Pyr<>Pyr photoproducts was detected.[1,6–10] It is, however, surprising that despite the importance of the matter just two recent high-level ab initio studies are available on this issue.[11,12] Those communications have independently suggested that the [2 + 2] cycloaddition photoreaction[13] for thymine (T) dimerization occurs via a barrierless concerted nonadiabatic mechanism on a singlet excited-state through a S_1/S_0 conical intersection (CI), which is the funnel for ultrafast nonradiative decay leading to T<>T.[11,12]

(1) Cadet, J.; Vigny, P. In *Bioorganic Photochemistry*; Morrison, H., Ed.; John Wiley & Sons: New York, 1990; Vol. 1, pp 1−272.
(2) Douki, T.; Cadet, J. *Biochemistry* **2001**, *40*, 2495–2501.
(3) Heelis, P. F.; Hartman, R. F.; Rose, S. D. *Chem. Soc. Rev.* **1995**, 289–297.
(4) Danilov, V. I.; Slyusarchuk, O. N.; Alderfer, J. L.; Stewart, J. J. P.; Callis, P. R. *Photochem. Photobiol.* **1994**, *59*, 125–129.
(5) Kraemer, K. H. *Proc. Natl. Acad. Sci. U.S.A.* **1997**, *94*, 11–14.
(6) Crespo-Hernández, C. E.; Cohen, B.; Hare, P. M.; Kohler, B. *Chem. Rev.* **2004**, *104*, 1977–2019.
(7) Crespo-Hernández, C. E.; Cohen, B.; Kohler, B. *Nature* **2005**, *436*, 1141–1144.
(8) Marguet, S.; Markovitsi, D. *J. Am. Chem. Soc.* **2005**, *127*, 5780–5781.
(9) Schreier, W. J.; Schrader, T. E.; Soller, F. O.; Gilch, P.; Crespo-Hernández, C. E.; Swaminathan, V. N.; Carell, T.; Zinth, W.; Kohler, B. *Science* **2007**, *315*, 625–629.
(10) Holman, M. R.; Ito, T.; Rokita, S. E. *J. Am. Chem. Soc.* **2007**, *129*, 6–7.
(11) Boggio-Pasqua, M.; Groenhof, G.; Schäfer, L. V.; Grubmüller, H.; Robb, M. A. *J. Am. Chem. Soc.* **2007**, *129*, 10996–10997.
(12) Blancafort, L.; Migani, A. *J. Am. Chem. Soc.* **2007**, *129*, 14540–14541.
(13) Klessinger, M.; Michl, J. *Excited States and Photochemistry of Organic Molecules*; VCH Publishers: New York, 1995.

10.1021/ja803068n CCC: $40.75

The major photoproduct induced in DNA by UV radiation is T<>T, but TT sites are not mutational hotspots.[2] In contrast, cytosine-cytosine (CC) sequences are sites of relatively frequent CC to TT tandem mutations, although the corresponding photoproducts (C<>C) are produced with relatively lower yields.[2] As a first step toward elucidating the distinct behavior of CC with respect to TT sites, we focus in this contribution on the characterization on theoretical grounds of the intrinsic mechanisms responsible for the production of cyclobutane cytosine (CBC) along both the triplet and singlet manifolds.

The nature of electronic excited states in base multimers depends on conformation and base sequence.[6–10,14–16] The electronic coupling between closely spaced bases is responsible for the distinct spectroscopic features such as the well-known hypochromism of the lowest-energy absorption band and the decrease of the ionization potential.[6,15] The coupling is not large enough, however, to affect significantly the absorption spectra of biopolymers. Thus, the DNA absorption spectrum closely resembles the sum of the spectra of its building blocks. For this reason, it is generally assumed that, when DNA is illuminated by UV radiation, light is initially absorbed by the nucleic acid bases leading mainly to excited states of the same multiplicity (singlet) as the respective ground state. The low-lying excited states of DNA bases that can be accessed by UV absorption lie near 5 eV.[6,15] Thanks to the great efforts of several groups during the last decades, together with the outstanding development of novel spectroscopic techniques seen more recently, it is well established by now the extremely short lifetimes, in the subpicosecond regime, of singlet excited states of nucleotides, nucleosides, and isolated purine and pyrimidine bases, suggesting the presence of fully operative ultrafast internal conversion (IC) channels.[6,9,14,17] Accordingly, the fluorescence quantum yields measured for these systems are small.[18] In the meantime, as a nice example of constructive interplay between quantum chemistry and experimental outcome, computational evidence has been able to successfully identify specific radiationless decay mechanisms in isolated DNA bases,[19–43] involving energetically accessible regions of so-called conical intersections (CIs) between the lowest excited and the ground state, which are essentially responsible for efficient internal conversion (IC).[13,44,45] These favorable IC processes represent a self-protection mechanism preventing the occurrence of chemical reactions induced by UV light. Photostability is therefore the primordial photophysical characteristic of the building blocks of DNA (as well as of their Watson−Crick canonical pairs[46]), a concomitant DNA property, crucial to understanding life on earth as we know it, that has probably evolved as the most optimal biochemical response of genetic material to sunlight exposure.

The fluorescence spectra of multimers are qualitatively different from that of the constituent nucleotides. The most striking photophysical attribute of base polynucleotides and DNA is the appearance of long-lived emissive states not found in base monomers. The red-shifted emission seen in base multimers was first termed *excimer fluorescence* by Eisinger et al.,[16] and it is observed for both the single- and double-stranded forms of polynucleotides. Eight years ago, Plessow et al.,[47] employing a novel picosecond laser approach, reported time- and wavelength-resolved fluorescence of different oligonucleotides and were able to make readily apparent the longer-decay components of the emission, that are assumed to have arisen from excimer formation. In this respect, we have recently reported that formation of bound cytosine excimers can be regarded as an intrinsic property of the cytosine dimer.[48] In particular, the computed vertical emission fully supports the excimer origin of the red-shifted fluorescence observed in cytosine-containing oligonucleotides.[16,47] A recent femtosecond excited-state absorption (fs-ESA) study of Kohler and coworkers[7] has shown that excimers are formed in high yields in a variety of synthetic DNA oligonucleotides and concludes that excited-state dynamics of A·T DNA is controlled by base stacking. On the other hand, Kwok et al.[14] have subsequently reported the first femtosecond combined time- and wavelength-resolved study on the ultraviolet-excited adenosine and a single-stranded adenine-containing oligonucleotide in aqueous solution,

(14) Kwok, W.-M.; Ma, C.; Phillips, D. L. *J. Am. Chem. Soc.* **2006**, *128*, 11894–11905.
(15) Eisinger, J.; Shulman, R. G. *Science* **1968**, *161*, 1311–1319.
(16) Eisinger, J.; Guéron, M.; Shulman, R. G.; Yamane, T. *Proc. Natl. Acad. Sci. U.S.A.* **1966**, *55*, 1015–1020.
(17) Canuel, C.; Mons, M.; Pluzzi, F.; Tardivel, B.; Dimicoli, I.; Elhanine, M. *J. Chem. Phys.* **2005**, *122*, 074316.
(18) Callis, P. R. *Annu. Rev. Phys. Chem.* **1983**, *34*, 329–357.
(19) Merchán, M.; Serrano-Andrés, L. *J. Am. Chem. Soc.* **2003**, *125*, 8108–8109.
(20) Merchán, M.; Serrano-Andrés, L.; Robb, M. A.; Blancafort, L. *J. Am. Chem. Soc.* **2005**, *127*, 1820–1825.
(21) Merchán, M.; González-Luque, R.; Climent, T.; Serrano-Andrés, L.; Rodríguez, E.; Reguero, M.; Peláez, D. *J. Phys. Chem. B* **2006**, *110*, 26471–26476.
(22) Serrano-Andrés, L.; Merchán, M.; Borin, A. C. *Chem. Eur. J.* **2006**, *12*, 6559–6571.
(23) Serrano-Andrés, L.; Merchán, M.; Borin, A. C. *Proc. Natl. Acad. Sci. U.S.A.* **2006**, 8691–8696.
(24) Climent, T.; González-Luque, R.; Merchán, M.; Serrano-Andrés, L. *Chem. Phys. Lett.* **2007**, *441*, 327–331.
(25) Matsika, S. *J. Phys. Chem. A* **2004**, *108*, 7584–7590.
(26) Kistler, K. A.; Matsika, S. *J. Phys. Chem. A* **2007**, *111*, 2650–2661.
(27) Marian, C. M. *J. Chem. Phys.* **2005**, *122*, 104314.
(28) Tomic, K.; Tatchen, J.; Marian, C. M. *J. Phys. Chem. A* **2005**, *109*, 8410–8418.
(29) Marian, C. M. *J. Phys. Chem. A* **2007**, *111*, 1545–1553.
(30) Perun, S.; Sobolewski, A. L.; Domcke, W. *J. Am. Chem. Soc.* **2005**, *127*, 6257–6265.
(31) Perun, S.; Sobolewski, A. L.; Domcke, W. *J. Phys. Chem. A* **2006**, *110*, 13238–13244.
(32) Ismail, N.; Blancafort, M.; Olivucci, M.; Kohler, B.; Robb, M. A. *J. Am. Chem. Soc.* **2002**, *124*, 6818–6819.
(33) Blancafort, L.; Cohen, B.; Hare, P. M.; Kohler, B.; Robb, M. A. *J. Phys. Chem. A* **2005**, *109*, 4431–4436.
(34) Blancafort, L. *J. Am. Chem. Soc.* **2006**, *128*, 210–219.
(35) Chen, H.; Li, S. H. *J. Phys. Chem. A* **2005**, *109*, 8443–8446.
(36) Chen, H.; Li, S. H. *J. Chem. Phys.* **2006**, *124*, 154315.
(37) Nielsen, S. B.; Sølling, T. I. *ChemPhysChem* **2005**, *6*, 1276–1281.
(38) Gustavsson, T.; Banyasz, A.; Lazzarotto, E.; Markovitsi, D.; Scalamani, G.; Frisch, M. J.; Barone, V.; Improta, R. *J. Am. Chem. Soc.* **2006**, *128*, 607–619.
(39) Zgierski, M. Z.; Patchkovskii, S.; Lim, E. C. *J. Chem. Phys.* **2005**, *123*, 081101.
(40) Zgierski, M. Z.; Patchkovskii, S.; Fujiwara, T.; Lim, E. C. *J. Phys. Chem. A* **2005**, *109*, 9384–9387.
(41) Zgierski, M. Z.; Patchkovskii, S.; Lim, E. C. *Can. J. Chem.* **2007**, *85*, 124–134.
(42) Serrano-Pérez, J. J.; González-Luque, R.; Merchán, M.; Serrano-Andrés, L. *J. Phys. Chem. B.* **2007**, *111*, 11880–11883.
(43) Serrano-Andrés, L.; Merchán, M.; Borin, A. C. *J. Am. Chem. Soc.* **2008**, *130*, 2473–2484.
(44) Olivucci, M., Ed. *Computational Photochemistry*; Elsevier: Amsterdam, 2005.
(45) Domcke, W., Yarkony, D. R., Köppel, H., Eds. *Conical Intersections*; World Scientific: Singapore, 2004.
(46) Sobolewski, A. L.; Domcke, W.; Hättig, C. *Proc. Natl. Acad. Sci. U.S.A.* **2005**, *102*, 17903–17906.
(47) Plessow, R.; Brockhinke, A.; Eimer, W.; Kohse-Höinghaus, K. *J. Phys. Chem. B* **2000**, *104*, 3695–3704.
(48) Olaso-González, G.; Roca-Sanjuán, D.; Serrano-Andrés, L.; Merchán, M. *J. Chem. Phys.* **2006**, *125*, 231102.

providing clear evidence for the involvement of excimers in the excited relaxation pathways of adenine nucleotides.

The singlet excimer has been suggested by some authors to be a precursor to photodimerization.[1,4] In this sense, thymine dimerization has recently been determined by Schreier et al.[9] to be an ultrafast reaction along the singlet manifold, although no thymine excimers could be recorded earlier.[7] Therefore, the excited-state dimerization reaction occurs in competition with internal conversion processes to the electronic ground state. The role of triplet states in DNA chemistry, in particular on the formation of Pyr<>Pyr,[49,50] has been highlighted since it was first suggested by Cadet and co-workers.[1] Despite the fact that triplet formation has a low quantum yield, the longer-lived triplet states are crucial in the photochemistry and photophysics of DNA components, since they induce cyclobutane dimers at the bipyrimidine sites under triplet photosensitization conditions.[1,50] Another way for triplet state Pyr-formation is also possible. As it has been documented in detail for cytosine,[20] uracil,[24] and thymine,[42] the lowest triplet state can be populated along the ultrafast internal conversion by an intersystem crossing (ISC) mechanism. Apparently in contrast, recent time-resolved studies of thymine dimer formation by Marguet and Markovitsi[8] show that direct excitation of $(dT)_{20}$ leads to cyclobutane thymine dimers (T<>T) in less that 200 ns with a remarkably absence of any triplet absorption from the transient spectra of the oligonucleotide. It is clear that the origin and mechanisms of both excimer and photodimer formation at the molecular level are controversial and poorly understood.

In this scenario, a model built on the basis of predictive quantum chemical computations seems timely in order to understand the underlying basics at the molecular level of these relevant photoreactions. In particular, theory can shed light on whether excimers can be considered precursors of cyclobutane pyrimidine dimers. For this purpose, a well-established and sound quantum chemical ab initio method, namely the complete-active-space self-consistent-field second-order perturbation theory (CASPT2)[51–55] as implemented in the MOLCAS 6.0 software,[56] in conjunction with extended one-electron basis sets, was used.

Methods and Computational Details

The basis set of atomic natural orbital (ANO) type with the primitive set C,N,O(10s6p3d)/H(7s3p), the ANO-S set,[57] contracted to C,N,O[3s2p1d]/H[2s1p] was used throughout. Geometry optimizations, minimum reaction paths (MEPs), and determination of hypersurface crossings were carried out initially at the CASSCF level. The active space comprises the same π system employed earlier for ground-state cytosine.[19] It represents in the dimer a total of 16 electrons distributed among 14 molecular orbitals (MOs), that is, all the π system except for the deep π orbital localized on the NH_2 fragment of each cytosine, which was treated as inactive. Dynamic electron correlation was subsequently taken into account perturbatively at the second-order level through the CASPT2 method.[51] In order to mimic the actual interaction of pyrimidines in DNA, geometry optimizations were initially performed within the constraints of the C_s symmetry, thus allowing for an effective and natural interaction of two cytosine molecules in the biologically relevant cis−syn stereoisomer. Seven active MOs in each of the irreducible representation a′ and a″ (16 active electrons) were used in C_s symmetry. At the optimized geometries, the energies were computed at the CASPT2 level with no symmetry restrictions (C_1 symmetry), since wave function symmetry breaking is a prerequisite to describe correctly the asymptotic limit for the lowest electronic singlet and triplet transition of the two moieties. It is said that the calculation breaks symmetry when the computed electronic wave function has lower symmetry than that implied by the nuclear coordinates (see, e.g., ref 58). For the computations in C_1 symmetry, two additional π MOs were also kept inactive, since the occupation number of the corresponding natural orbitals when they were treated as active was practically 2.0. They correspond to the plus and minus linear combinations of the deeper all-in-phase π MOs of the two cytosine molecules. A CASSCF wave function of 12 active π electrons and 12 active π MOs was therefore employed, hereafter denoted as CASSCF(12,12). On the other hand, the corresponding results with the second-order corrections included shall be labeled as CASPT2(12,12). For the triplet and singlet states the state-average CASSCF(12,12) reference wave function involved two and four roots, respectively. In order to minimize weakly interacting intruder states, the imaginary level-shift technique with a parameter 0.2 au, has been employed.[59] MEPs have been built as steepest descendent paths in a procedure[60] which is based on a modification of the projected constrained optimization (PCO) algorithm of Anglada and Bofill[61] and follows the Müller−Brown approach.[62] Each step requires the minimization of the potential energy hypersurfaces on a hyperspherical cross section of the explored hypersurface centered on the initial geometry and characterized by a predefined radius. The optimized structure is taken as the center of a new hypersphere of the same radius, and the procedure is iterated until the bottom of the energy surface is reached. Mass-weighted coordinates are used, therefore the MEP coordinate corresponds to the so-called intrinsic reaction coordinate (IRC), measured in au, that is, bohr·amu$^{1/2}$. The singlet−triplet crossing $(T_1/S_0)_X$ and the conical intersection $(S_1/S_0)_{CI}$ were computed by using the restricted Lagrange multipliers technique as included in the MOLCAS-6.0 package[56] in which the lowest-energy point was obtained under the restriction of degeneracy between the two considered states.[60] The CASSCF structure computed for $(T_1/S_0)_X$ represents also a crossing at the CASPT2 level. It does not hold true for $(S_1/S_0)_{CI}$. Thus, the reported CASPT2 $(S_1/S_0)_{CI}$ conical intersection was obtained by exploring a grid of points along the distortions that involve the smallest values for the CASSCF gradients in the region of the crossing. Additional details on the computational strategy developed will be given in the next section as required.

As shown previously,[48] the inclusion of the basis set superposition error (BSSE) is crucial to accurately describe the binding energies. Here the effect was taken into account by using the

(49) Word, P. D.; Redmond, R. W. *J. Am. Chem. Soc.* **1996**, *118*, 4256–4263.
(50) Bosca, F.; Lhiaubet-Vallet, V.; Cuquerella, M. C.; Castell, J. V.; Miranda, M. A. *J. Am. Chem. Soc.* **2006**, *128*, 6318–6319.
(51) Andersson, K.; Malmqvist, P.-Å.; Roos, B. O. *J. Chem. Phys.* **1992**, *96*, 1218–1226.
(52) Serrano-Andrés, L.; Merchán, M.; Nebot-Gil, I.; Lindh, R.; Roos, B. O. *J. Chem. Phys.* **1993**, *98*, 3151–3162.
(53) Roos, B. O.; Andersson, K.; Fülscher, M. P.; Malmqvist, P.-Å.; Serrano-Andrés, L.; Pierloot, K.; Merchán, M. *Adv. Chem. Phys.* **1996**, *93*, 219–331.
(54) Merchán, M.; Serrano-Andrés, L. In *Computational Photochemistry*; Olivucci, M., Ed.; Elsevier: Amsterdam, 2005.
(55) Serrano-Andrés, L.; Merchán, M. In *Encyclopedia of Computational Chemistry*, Schleyer, P. v. R., Schreiner, P. R., Schaefer, H. F., III, Jorgensen, W. L., Thiel, W., Glen, R. C., Eds.; Wiley: Chichester, 2004.
(56) Andersson, K.; et al. *MOLCAS*, version 6.4; Department of Theoretical Chemistry, Chemical Centre, University of Lund: Lund, Sweden, 2006.
(57) Pierloot, K.; Dumez, B.; Widmark, P.-O.; Roos, B. O. *Theor. Chim. Acta* **1995**, *90*, 87–114.
(58) Merchán, M.; Pou-AméRigo, R.; Roos, B. O. *Chem. Phys. Lett.* **1996**, *252*, 405–414.
(59) Forsberg, N.; Malmqvist, P.-Å. *Chem. Phys. Lett.* **1997**, *274*, 196–204.
(60) De Vico, L.; Olivucci, M.; Lindh, R. *J. Chem. Theory Comput.* **2005**, *1*, 1029–1037.
(61) Anglada, J. M.; Bofill, J. M. *J. Comput. Chem.* **1997**, *18*, 992–1003.
(62) Müller, K.; Brown, L. D. *Theor. Chim. Acta* **1979**, *53*, 75–93.

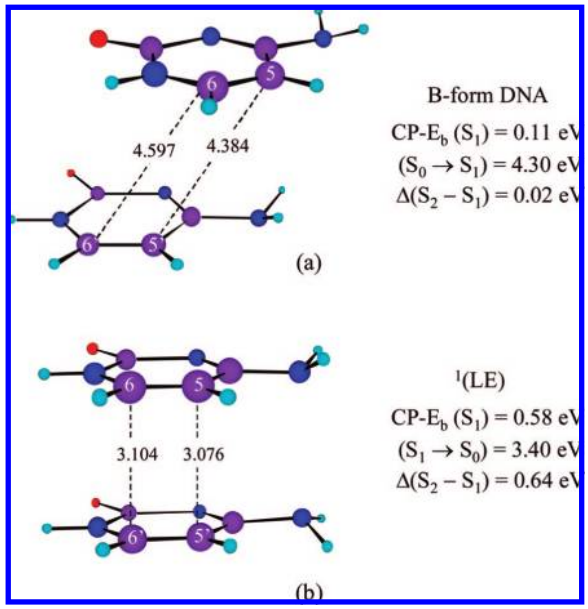

Figure 1. Structures for two cytosine molecules at the ground-state B-form DNA (a) and at the S_1 locally excited state ^{1}(LE)-type structure in a face-to-face orientation (b) (see text). The computed CASPT2 binding energies for S_1 corrected for the BSSE through the counterpoise correction, CP-E_b, the vertical absorption transition energy ($S_0 \rightarrow S_1$), the vertical fluorescence ($S_1 \rightarrow S_0$), together with the splitting for the two lowest excited states, $\Delta(S_2-S_1)$, are also included. Interatomic distances in Å.

counterpoise correction (CP).[63] The binding energy and the corrected counterpoise binding energy will be denoted E_b and CP-E_b, respectively (see Supporting Information).

All the computations have been carried out by using the MOLCAS 6.0 quantum-chemical software.[56]

Results and Discussion

Singlet and Triplet Cytosine Excimers. Figure 1 shows two cytosine molecules in the ground-state B-type DNA conformation[64] and the structure for the locally excited-state relative minimum on S_1, hereafter ^{1}(LE), computed at the CASPT2 level with respect to the intermolecular distance in the face-to-face π-stacked arrangement of the two moieties, maintaining the monomers at the optimized ground-state CASSCF(8,7) geometry.[48]

As can be readily seen from the molecular drawings, the ground-state stacking in the B-form is somewhat different from the idealized "sandwich" geometry required for producing a fully stabilized "excimer".[65] In the ground-state B-form DNA, the interatomic distances $R(C_5-C_{5'})$ and $R(C_6-C_{6'})$ are about 1.5 and 1.3 Å larger than those in ^{1}(LE), whereas the dihedral angle $\angle C_5-C_6-C_{6'}-C_{5'}$ varies from 0° in ^{1}(LE) to 38.6° in B-DNA. *The lowest singlet excited-state in the parallel excimer ^{1}(LE) is 0.47 eV more stable than in the B-form.* Accordingly, the binding energy (CP-E_b) for the former, ^{1}(LE), increases considerably, about half an eV, with respect to the B-form. In the B-form the vertical S_1 state is weakly bound, just by 0.11 eV, whereas the S_2-S_1 splitting is small, reflecting a weak coupling between the states. As expected, the vertical transitions, 4.30 eV (S_1) and 4.32 eV (S_2), are slightly red-shifted as compared to the lowest vertical singlet−singlet transition of the cytosine monomer. At the same level of theory, the ground-state CP-E_b in the B-form is computed to be 0.04 eV, whereas it is found −0.43 eV at the ^{1}(LE)-geometry. In fact, the potential energy curve with respect to the intermolecular distance of two cytosine molecules in the face-to-face orientation has been shown for the ground-state to be repulsive.[48] The vertical emission, calculated at the ^{1}(LE) structure, 3.40 eV, is consistent with the maximum of the red-shifted fluorescence observed for dinucleotides, polynucleotides, and DNA (3.2−3.4 eV).[16,47] On the other hand, the pronounced S_2-S_1 gap for ^{1}(LE), 0.64 eV, points out to an efficient coupling between the two states. Although at the ^{1}(LE) geometry the S_2 becomes unbound by 0.06 eV, the potential energy curve for the S_2 state has a minimum at longer interatomic distances.[48]

Taking into account the inherent flexibility of DNA and related oligonucleotides, competitive ^{1}(LE)-type orientations might be present at the time of UV-irradiation. Because of the concomitant increased stability in the lowest singlet excited-state at those parallel arrangements, geometries around the ^{1}(LE)-type structure can be considered the best candidates as precursors of photodimers. It seems that the ideal twist angle between successive base pairs makes the geometry of B-DNA (and A-DNA) nonreactive. According to recent experimental evidence,[9] the static Pyr-Pyr conformations and not conformational motions after photoexcitation determines the formation of Pyr<>Pyr photoproducts. Within the model proposed by Schreier et al.,[9] the relatively smaller degree of flexibility of A-DNA compared to B-DNA to achieve the right orientations that become prone to react can be related to the greater resistance of A-DNA to Pyr<>Pyr formation. As shown by these authors, dimerization occurs only for thymine residues that are already in a reactive arrangement at the instant of excitation, because the rate of photoproduct formation by favorably oriented thymine pairs is much faster that the rate of orientation change. A similar situation can therefore be assumed in cytosine oligomers. From the results compiled so far, the ^{1}(LE)-type cytosine excimer is revealed as a reactive intermediate, a possible source of the CBC photoproduct, and consequently the ^{1}(LE) excimer has been taken as the starting point for the study of the dimerization reaction occurring along the singlet manifold (see below). It is also worth pointing out that singlet cytosine excimers may be involved in the photoinduced formation of the pyrimidine 6-4 pyrimidone photoadducts (Pyr(6-4)Pyr), whose precursor is an oxetane adduct, and other minor photohydrated products.[1] For cytosine in particular, and in contrast to cellular DNA, in the isolated system the formations of C<>C and C(6-4)C become competitive.[2] For a complete elucidation of the relative importance of those mechanisms, modeling of the environment and explicitly considering the Watson−Crick pairing should be most probably required since the yield formation depends on the type of nucleotide, the isolated or cellular nature of the DNA biopolymer, and the range of the UV radiation.[8,9,66,67] Future research shall be addressed in those directions.

A parallel study has been performed for the two lowest triplet states. The numerical results are listed in Table 1, where for the sake of completeness the related findings for the two lowest singlet excited states are also included. The potential energy curves at the CASPT2(12,12)+BSSE level are depicted in Figure 2. The corresponding BSSE-uncorrected results can be

(63) Boys, S. F.; Bernardi, F. *Mol. Phys.* **2002**, *100*, 65–73.
(64) Lu, X.-J.; Olson, W. K. *Nucleic Acids Res.* **2003**, *31*, 5108–5121.
(65) Birks, J. B. *Rep. Prog. Phys.* **1975**, *38*, 903–974.
(66) Douki, T.; Court, M.; Sauvaigo, S.; Odin, F.; Cadet, J. *J. Biol. Chem.* **2000**, *275*, 11678–11685.
(67) Mouret, S.; Baudouin, C.; Charveron, M.; Favier, A.; Cadet, J.; Douki, T. *Proc. Natl. Acad. Sci. U.S.A.* **2006**, *103*, 13765–13770.

Table 1. Binding Energy (E_b), Basis Set Superposition Error (BSSE) Obtained through the Counterpoise Method (CP-BSSE), and Corrected Binding Energy CP-E_b, Computed at the CASPT2(12,12) Level for the Lowest Triplet and Singlet Excited States of the Cytosine Excimer[a]

state	$R(C_5-C_{5'})$	E_b[b]	CP-BSSE	CP-E_b
At the $(T_1)_{min}$ Structure:				
T_1	3.029	1.15	0.98	0.17
S_0	3.029	0.41	0.97	−0.56
vertical emission[c]: 2.93 eV (=3.66−0.17−0.56)				
0−0 transition[c]: 3.49 eV (=3.66−0.17)				
At the $(T_1)_{min}$+BSSE structure: ^{3}(LE)				
T_1	3.304	1.06	0.84	0.22
S_0	3.304	0.61	0.82	−0.21
vertical emission[c]: 3.23 eV (=3.66 - 0.22 - 0.21)				
0−0 transition[c]: 3.44 eV (=3.66−0.22)				
At the $(S_1)_{min}$ Structure:[d]				
S_1	2.954	1.51	0.97	0.54
S_0	2.954	0.29	0.97	−0.68
vertical emission[c] S_0 S_1: 3.19 eV[d] (=4.41−0.54−0.68)				
0−0 transition[c]: 3.87 eV (=4.41−0.54)				
At the $(S_1)_{min}$+BSSE Structure: ^{1}(LE)				
S_1	3.076[d]	1.47	0.89	0.58[d]
S_0	3.076	0.47	0.90	−0.43
vertical emission[c]: 3.40 eV[d] (=4.41−0.58−0.43)				
0−0 transition[c]: 3.83 eV (=4.41−0.58)				

[a] Distances in Å and energies in eV. The triplet and singlet locally excited states ^{3}(LE) and ^{1}(LE) discussed in the text are identified. [b] Binding energy with respect to the corresponding states of the monomers. [c] Vertical excitations in the monomer: $S_0 \rightarrow T_1$ (3.66 eV) and $S_0 \rightarrow S_1$ (4.41 eV). [d] Taken from Olaso-González et al.[48]

found in the Supporting Information. The accurate theoretical treatment of these singlet and triplet excimers becomes particularly challenging since it requires inclusion of electron dynamic correlation, flexible enough one-electron basis sets, wave functions with no symmetry constraints in order to achieve the correct asymptotic limit, and BSSE corrections. The influence of the latter factor is apparent by inspection and comparison of the two sets of results displayed in Figure 2 and in the Supporting Information.

At the highest level of theory employed, the binding energy for the lowest triplet state (T_1) computed at the CASPT2(12,12)+BSSE level is 0.22 eV, with a predicted vertical emission (phosphorescence) of 3.23 eV and a 0−0 triplet−singlet transition of 3.44 eV. Consequently, it is concluded that the triplet excimer is bound, although the binding energy is reduced about 60% with respect to the lowest singlet excimer. Interestingly, as can be noted from Figure 2, the S_1 and T_2 states are involved in a singlet−triplet crossing around the intermolecular distance 3.0−3.4 Å, precisely the distances expected for the ground-state biopolymer.[6,15] Thus, T_2 could be populated through an ISC mechanism, becoming then deactivated toward T_1 via a CI facilitated with the breathing movement of the own DNA. Apart from the near-degeneracy found, the magnitude of the spin−orbit coupling (SOC) is also relevant to asses the efficiency of the ISC process, which would be strongly affected by the actual environment of the biopolymer. The possibility of excimer formation arises from the Watson−Crick structure in which hydrogen-bonded pairs A-T and G-C are situated inside a double helix, the backbone formed by two sugar-phosphate chains. One turn of the helix involves 10 base pairs and is 34 Å high. Thus, the interplanar distance between neighboring base pairs is about 3.4 Å, a value which is often found in excimer-type organic crystals.[65,68] The structure for the locally excited-state relative minimum on T_1 computed at the CASPT2(12,12)+BSSE level with respect to the intermolecular distance in the face-to-face arrangement (maintaining the monomers at the optimized ground-state geometry) shall be accordingly denoted as ^{3}(LE). As compiled in Table 1, the ^{3}(LE) structure has a $R(C_5-C_{5'})$ distance of 3.304 Å. Similarly, as in the case of the singlet manifold, the ^{3}(LE)-type cytosine excimer has been taken as the starting structure to study the intrinsic reactivity of the system along the triplet manifold.

To summarize, from the results compiled so far, the ^{1}(LE)- and the ^{3}(LE)-type cytosine excimers are revealed as promising, local, two-by-two reactive intermediates easily accessible in DNA single- and double strands that may be the source of the CBC dimer photoproducts, and consequently they have been taken as the starting point for the study of the photoinduced dimerization reaction occurring along the singlet and triplet manifold, respectively. Of course, the LE-type structures might not be the unique arrangements susceptible of initiating photoreactions in such complex hypersurfaces, but a priori they are clear candidates and bear the requirements to produce C<>C, and we shall therefore focus next on how they evolve. In fact, as shall be discussed below, the T_1-MEP and S_1-MEP computations from the ^{3}(LE) and ^{1}(LE) structures lead to stationary points on the respective hypersurfaces close to regions where an efficient radiationless decay toward the ground state can take place.

Photodimerization of Cytosine along the Triplet Manifold. A detailed analysis of the CASSCF wave functions for the LE states, that is, the T_1 and S_1 states at the LE geometries, shows that both the triplet ^{3}(LE) and the singlet ^{1}(LE) excited states can be described as belonging to the irreducible representation $^{3,1}A''$, as appropriate, of the C_s symmetry group. The CASPT2 energies for the states ^{3}(LE) and ^{1}(LE) computed within the geometrical constraints of C_s and with no restrictions (C_1 symmetry) are actually the same. In other words, no symmetry breaking of the respective wave functions is made apparent at the geometries of the ^{3}(LE) and ^{1}(LE) states as it happens markedly when going to longer intermolecular distances of the two cytosine moieties. In fact, only working in C_1 symmetry the degeneracy between the two lowest triplet (T_2, T_1) and singlet (S_2, S_1) states can be achieved at the asymptotic limit (cf. Figure 2). Inspired by this finding, CASSCF geometry optimizations and MEP computations for the lowest triplet and singlet states were carried out in practice for the $^{3,1}A''$ states (C_s symmetry). In order to make sure that a balanced treatment is given in all the explored regions of the hypersurfaces considered, the CASPT2 results reported here correspond always to computations carried out in C_1 symmetry. Furthermore, consistency with the results presented for the excimers in the previous section requires also inclusion of the BSSE correction. Therefore, BSSE has been introduced in the calculation of the relative stability between the different structures discussed. This is an important remark to bear in mind, because as the structural difference between two given stationary points becomes larger, the larger the difference between the computed relative stability with or without the BSSE correction would be. The procedure is certainly somewhat cumbersome, but it has the advantage that the results obtained for the states are consistent and directly comparable among them at the distinct geometries, from CBC to infinity separation of the two cytosine molecules.

(68) Klöpffer, W. In *Organic Molecular Photophysics*; Birks, J. B., Ed.; Interscience: London, 1973; pp 357−402.

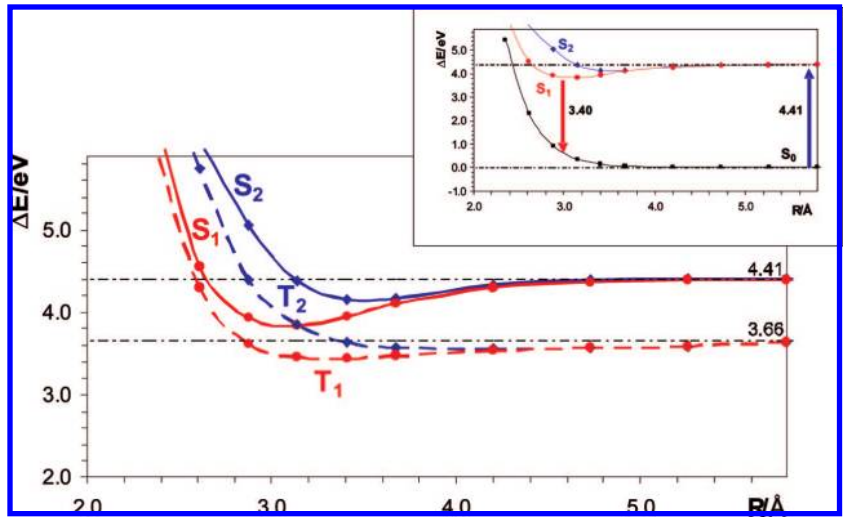

Figure 2. CASPT2+BSSE potential energy curves built with respect to the intermolecular distance $R(C_5-C_{5'})$ of two face-to-face π-stacked cytosine molecules involving the ground and the lowest two triplet and two singlet excited states. The inset, obtained at the same level of theory,[48] illustrates the emission event related to the observed red-shifted fluorescence in cytosine oligonucleotides.[16,47]

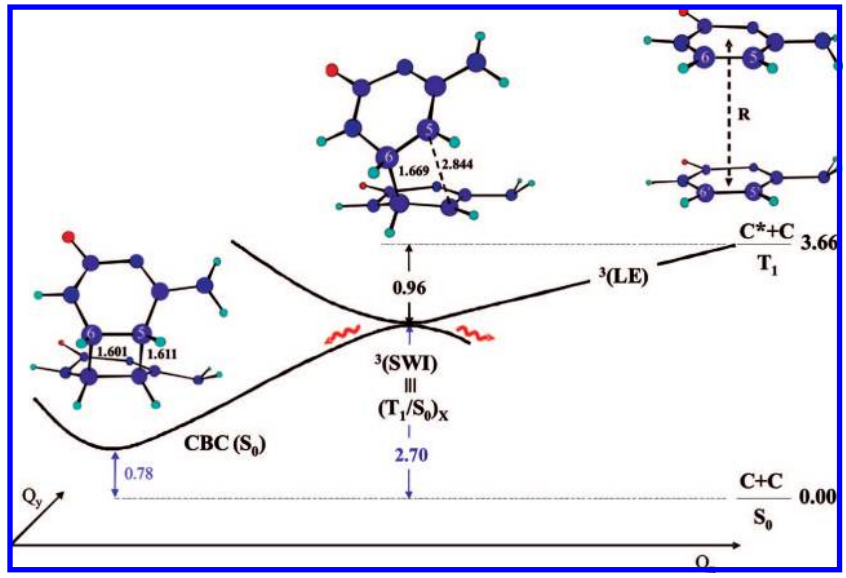

Figure 3. Proposed scheme, based on actual CASPT2 results, for the decay path of the lowest triplet excited state (T_1) of the cytosine dimer through the triplet locally excited state ^{3}(LE) and the stepwise intermediate ^{3}(SWI) leading to ground-state cyclobutane cytosine (CBC) via an intersystem crossing mechanism (ISC). The main intermolecular geometric parameters (in Å) are included. The remaining numerical values (in eV) correspond to relative energies, as indicated, with respect to two ground-state cystosine molecules separated by $R \cong 10.5$ Å. At the ^{3}(SWI)-optimized structure a singlet−triplet crossing, $(T_1/S_0)_X$, takes place. The Q_x coordinate is mainly related to the average intermolecular distance of $R(C_5-C_{5'})$ and $R(C_6-C_{6'})$, whereas Q_y is associated to the remaining degrees of freedom.

The overall proposed photodimerization decay path taking place along the triplet manifold is shown schematically in Figure 3. On the right-hand side of Figure 3, C + C denote two ground-state cytosine molecules separated by about 10.5 Å, both at the equilibrium geometry of ground-state cytosine. In C* + C one monomer (C*) is electronically excited. Transition from the ground to the lowest excited-state at this intermolecular distance thus corresponds to the vertical transitions $S_0 \rightarrow T_1$, 3.66 eV, in agreement with earlier results for isolated cytosine.[20] The CASPT2 results for the MEP computation along the T_1 state starting from the ^{3}(LE) state are depicted in Figure 4, where the evolution of the S_0 and T_2 states is also included. Remarkably, the T_1-MEP leads directly in a barrierless fashion to a structure coincident to that obtained by optimizing the geometry, denoted as a triplet stepwise intermediate, ^{3}(SWI), which has a clear degeneracy with the ground state. In other words, the triplet state is coincident with a triplet−singlet crossing, $(T_1/S_0)_X$, a region of the hypersurface where decay to the ground state becomes particularly favored.

The stationary point ^{3}(SWI) is characterized by the formation of a single covalent bond between the $C_6-C_{6'}$ atoms computed to be 1.669 Å, whereas the $C_5-C_{5'}$ interatomic distance stays elongated, about 2.8 Å (see Figure 3). Thus, ^{3}(SWI) cannot be really considered an excimer but an intermediate toward the formation of CBC.

Starting from an ample range of parallel arrangements around the ^{3}(LE) structure, geometry optimization of the ^{3}A″ state leads unambiguously to the ^{3}(SWI) structure, pointing out to the presence of many related reactive orientations. Of course, if the symmetry restrictions are released and initially the two cytosine molecules are considerably far apart, at about an intermolecular distance of 7 Å or larger, a local relaxed triplet in one of the

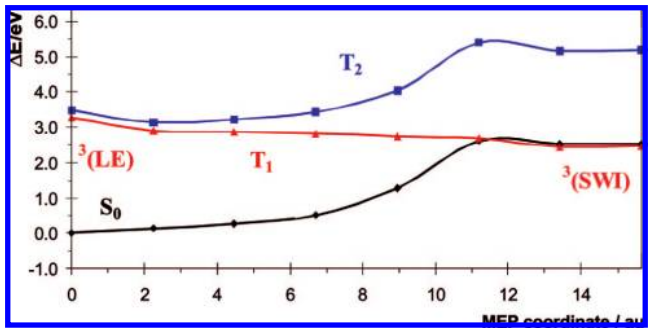

Figure 4. Low-lying triplet excited states of the cytosine dimer computed at the CASPT2//CASSCF level along the minimum energy path (MEP) of the T_1 state from the geometry of the triplet locally excited state ^{3}(LE). The T_1-MEP ends at the stepwise intermediate ^{3}(SWI) (see Figure 3), and it is isoenergetic with the ground state (S_0).

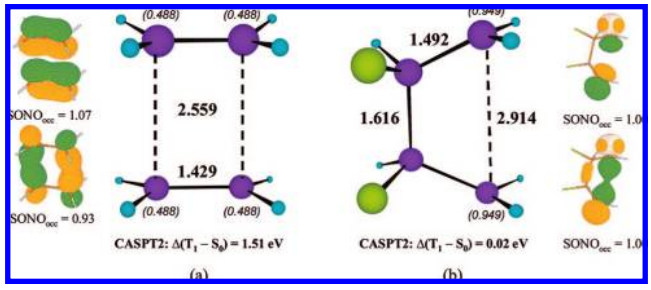

Figure 5. CASSCF(4,4) optimized geometry for the lowest triplet state of the ethene dimer (a) and the fluorethene dimer (b). The occupation number of the corresponding CASSCF singly occupied natural orbital ($SONO_{occ}$) is also included, as well as the CASPT2(4,4) energy difference computed between the lowest triplet and ground state. Main spin population derived from Mulliken analysis is given within parentheses. Distances in Å.

monomers is obtained, whereas the other maintains the ground-state equilibrium structure. As documented in detailed elsewhere,[20] the lowest triplet state of the monomer has $\pi\pi^*$ character and a band origin of 3.04 eV, which represents an stabilization of about 0.6 eV with respect to the vertical singlet−triplet transition.

In order to get further insight into the source and nature of the species ^{3}(SWI), comparable results for the lowest triplet state of ethene and fluorethene dimers (ED and FED hereafter) are helpful and illustrative. The T_1 state for ED and FED has been optimized at the CASSCF(4,4) level employing as active space the π valence molecular orbitals (MOs) (four electrons active) and the same ANO-type basis set as for cytosine. As can be readily seen from Figure 5, the equilibrium geometry for the lowest T_1 state of the FED molecule resembles to that of ^{3}(SWI), whereas for ED the structure of lowest T_1 state (HOMO−LUMO type) is rectangular. Furthermore, the single bond formed in T_1 of FED involves the intermolecular substituted carbon atoms, and the spin density is localized on the remaining carbon atoms. The T_1-FED equilibrium structure corresponds clearly to a biradical, and not surprisingly, it is degenerate with the ground state, both at the CASSCF and CASPT2 levels. On the contrary, for ED the T_1 state is about 1.5 eV above S_0, having the spin density of the two unpaired electrons equally shared by the four carbon atoms. Interestingly, according to the nature of the states, the optimized geometries for T_1-ED and T_1-FED are actual minima. A similar situation can be expected for ^{3}(SWI) in the cytosine dimer.

The singlet−triplet degeneracy occurring at the equilibrium structure ^{3}(SWI) can be therefore understood on the basis of the biradical character of the triplet/singlet states, having the unpaired electrons located on the C_5 and $C_{5'}$ atoms, yielding also a rationalization for the relatively longer $C_5-C_{5'}$ bond distance with respect to that calculated for $C_6-C_{6'}$. Taking into consideration that the C_6 atom (and $C_{6'}$) is attached to a nitrogen atom, whereas C_5 (and $C_{5'}$) is linked to a carbon atom, the C_6 and $C_{6'}$ centers are relatively more electron deficient than the C_5 and $C_{5'}$ atoms, since the electron affinity of nitrogen is higher than that of carbon. The single bond-making process between C_6 and $C_{6'}$ is therefore favored. As it occurs in FED, the substituted carbon atoms compensate for the lack of electron density by getting closer to the other monomer, causing in their quest for restoring the missed electron density the birth of a new bond.

The ^{3}(SWI) state has a CP-E_b of 0.96 eV and lies 2.70 eV above two ground-state cytosine molecules, which represents a stabilization of 0.3 eV with respect to the adiabatic triplet state of isolated cytosine. The 2.70 eV energy can be considered a lower bound for the triplet energy of cytosine in DNA. It can be envisaged that exogenous photosensitizers would populate the relaxed triplet state of the monomer, which may interact attractively with ground-state cytosine, and the so-formed dimer would evolve toward ^{3}(SWI), precursor of CBC. The possibility of endogenous photosensitization by triplet energy transfer in DNA between different nucleobases has also to be kept in mind. In either case, the required energy to access the ^{3}(SWI) state can be related to the threshold observed experimentally in a given compound to become a potential DNA photodamager via C<>C formation. The computed result for the ^{3}(SWI) state of cytosine, 2.70 eV, is consistent with the triplet energy of thymine in DNA deduced experimentally, 2.80 eV.[50] Triplet−triplet energy transfer is very important and common in chemical reactions.[13] It is utilized to specifically populate the triplet state of the reactant. This process is referred to as photosensitization, and the donor is called a triplet sensitizer. It is important to recall that, for efficient energy transfer to take place, the donor must absorb in the region of interest, undergo efficient ISC, and have a triplet-state energy higher than that of the acceptor, that is in this case, the ^{3}(SWI) species. The present results offer a nice rationale to the known fact that pyrimidine dimers are formed in solution under triplet photosensitization conditions.[1]

The computed intermediate ^{3}(SWI) thus represents a channel for photodimer formation from the triplet state of π-stacked cytosine in DNA and provides the basic understanding of potential phototogenotoxicity via triplet−triplet sensitization. It is known that UVA radiation (3.10−3.87 eV) preferentially induces the production of cyclobutane dimers at TT sites without any detectable formation of Pyr(6-4)Pyr photoproducts. Direct singlet population cannot take place at such low irradiation energies, and the process should then proceed through a triplet-energy transfer photosentization mechanism.[67] As preliminary calculations support, a similar pathway for the formation of the ^{3}(SWI) intermediate can be expected to take place for dimers including thymine. At higher irradiation energies, UVB or UVC, the singlet excited states of the pyrimidine molecule are accessible, and the mechanism of intrinsic population of the lowest triplet state of the monomer becomes operative. Since the efficiency of triplet-state formation has been determined to be larger in isolated thymine than in cytosine,[20,42] it is possible to rationalize the preference of the TT sites, and to a lesser extent CT, TC, and CC, to generate the cyclobutane photoproduct.

The presence of the $(T_1/S_0)_X$ crossing clearly favors the ISC to the ground state, but the actual efficiency of the decay process

along the triplet manifold will also rely on the enhancement of the SOC, estimated to be just a few cm^{-1} at the in-vacuo ^{3}(SWI) structure. In this respect, the solvent (or, in general, the environment) is expected to play a crucial role in the ISC process.[69] Under favorable ISC conditions, the decay would most probably take place on a subpicosecond range, which is considerably less than the 200 ns employed in the time-resolved study of thymine dimer formation.[8] We support therefore the suggestion made by Marguet and Markovitsi[8] in relation to the possibility that the ultrafast reactivity of the triplet state to yield cyclobutane dimers occurs with quasi-unit efficiency.

Photodimerization of Cytosine along the Singlet Manifold. Considering the seminal work reported by Bernardi, Olivucci, and Robb in 1990 on predicting forbidden and allowed excited-state [2 + 2] cycloadditon reactions of two ethene molecules, decay toward ground-state CBC from the singlet excimer should take place via a CI.[70,71] The ethene−ethene photochemical cycloaddition reaction path has been documented to occur in a single step via a rhomboid (C_{2h} symmetry) conical intersection,[72] and a similar situation is expected to occur here as it has already been documented for the thymine dimer.[11,12] Imposing C_s symmetry in the study represents therefore a clear approximation in this case, since in principle the rhomboid arrangement cannot be reached. The cut along the singlet reaction path within C_s symmetry would lead to a region of the S_1 surface used to be referred as "pericyclic minimum" because it was thought that, in general, the touching between the states was likely weakly avoided everywhere, even without symmetry constraints.[13] Thanks to the extensive work performed by these authors and many others,[44,45] the exact location of the bottom of the respective funnel has been determined in considerable detail for many different processes and has been demonstrated to be of fundamental significance in many photoreactions. In this respect, it should be emphasized that exploring the excited-state potential energy surfaces by using geometries from the ground-state path might lead to meaningless results, and consequently, the model should not be employed. Currently, the importance of the crucial role played by CIs in modern photochemistry is well established theoretically and supported experimentally.

If one is able to connect the different relevant stationary points to CBC within C_s symmetry constraints, the geometry around the touching region would be then a good guess for the computation of the actual CI (C_1 symmetry). The computational strategy has been found quite advantageous, especially taking into consideration that the present study is addressed to get further insight into the intrinsic possible photodimerization paths along the singlet manifold occurring in oligonucleotides and DNA. The C_s symmetry constraints somehow simulate for two cytosine monomers the restrictions that those would have in the actual biopolymer. In order to be fully aware of the complexity of the study, it is worth mentioning that unconstrained geometry optimization of two stacked cytosine molecules leads for the lowest singlet states to structures with orientations unlikely to occur in the single and double strands of DNA. Those unconstrained structures are solely appropriate to be compared to the gas-phase data, a target that is out of the scope of the current research and shall not be further discussed. Past work has overcome this problem by keeping fixed the $C_5-C_{5'}$ and $C_6-C_{6'}$ bonds and the corresponding dihedral angle to those data known for a B-DNA form.[11,12,73,74] For the reasons indicated above, we have first preferred mapping the full photoreaction within C_s symmetry, which nicely gives the basic clues of the nonradiative decay path taking place along the S_1 hypersurface toward the ground state.

On the basis of CASPT2 results, the overall photoinduced production of CBC along the singlet manifold is schematically displayed in Figure 6. On the right-hand side of the drawing, the transition $S_0 \rightarrow S_1$ at 4.41 eV corresponds to that of the isolated cytosine molecule. The related oscillator strength for the singlet−singlet absorption is 0.09. The findings are consistent with earlier results for the system at the same level of theory.[19,21,48] Using a similar notation as in Figure 3, C + C represent two ground-state cytosine molecules separated at about 10.5 Å, both at the equilibrium geometry of ground-state cytosine, whereas in C* + C one monomer (C*) is in the lowest electronically excited (singlet, in Figure 6) state. As shown in Figure 7, MEP computations along the singlet excited state starting from the ^{1}(LE) excimer leads in a barrierless form to a relaxed excimer, hereafter labeled like ^{1}(C*C). In the MEP ^{1}(LE) - ^{1}(C*C) the energy of the ground-state is not significantly affected (cf. Figure 7). Recall at this point that CASSCF MEP geometry optimizations were carried out within C_s symmetry for the $1^1A''$ state, and punctual CASPT2 calculations at the converged structures were obtained from averaging the lowest four roots with no symmetry constraints. As it is clearly verified from Figure 8, the relaxed excimer ^{1}(C*C) connects with the lowest singlet excited-state of the photodimer CBC, and it is apparent that from ground-state CBC the S_1-MEP evolves in a steepest descendent fashion toward the relaxed structure ^{1}(C*C). For the sake of completeness, results for the S_2 and S_3 states are also included in Figures 7 and 8. For CBC, the lowest vertical transition, computed to be at 4.57 eV with oscillator strength 0.070, is expected to contribute to the photoreversibility process observed in pyrimidines.[10] The energy of the ground state (S_0) along the S_1-MEP of Figure 8 increases progressively and, after reaching a maximum, decreases. Around the proximity of the MEP coordinate 4.5 au where the maximum for S_0 is accomplished, the S_1 and S_0 states are placed relatively close, being the corresponding geometry a good candidate as initial trial to search for a crossing between the respective singlet hypersurfaces. In this manner, the stationary point for the actual conical intersection $(S_1/S_0)_{CI}$ displayed in Figure 6 was obtained in C_1 symmetry. The funnel $(S_1/S_0)_{CI}$ provides the 2-fold channel for ultrafast internal conversion toward the ground-state of the system, that is, to CBC and to the separated monomers, although just the former has been emphasized in Figure 6.

The relaxed excimer ^{1}(C*C) has a binding energy (CP-E_b) of 1.10 eV, and it is stabilized with respect to ^{1}(LE) by about ~0.5 eV. In order to reach the conical intersection $(S_1/S_0)_{CI}$ from ^{1}(C*C), the system has to surmount a barrier height of 0.2 eV. Because of the pronounced CP-E_b and the presence of a barrier, the relaxed species ^{1}(C*C) can be expected to be fluorescent. The predicted fluorescence features from ^{1}(LE) and ^{1}(C*C), 3.40 and 2.76 eV, respectively, may help to rationalize

(69) Hare, P. M.; Crespo-Hernández, C. E.; Kohler, B. *J. Phys. Chem. B* **2006**, *110*, 18641–18650.
(70) Bernardi, F.; De, S.; Olivucci, M.; Robb, M. A. *J. Am. Chem. Soc.* **1990**, *112*, 1737–1744.
(71) Bernardi, F.; Olivucci, M.; Robb, M. A. *Acc. Chem. Res.* **1990**, *23*, 405–412.
(72) Celani, P.; Robb, M. A.; Garavelli, M.; Bernardi, F.; Olivucci, M. *Chem. Phys. Lett.* **1995**, *243*, 1–8.
(73) Durbeej, B.; Eriksson, L. A. *Photochem. Photobiol.* **2003**, *78*, 159–167.
(74) Zhang, R. B.; Eriksson, L. A. *J. Chem. Phys. B* **2006**, *110*, 7556–7562.

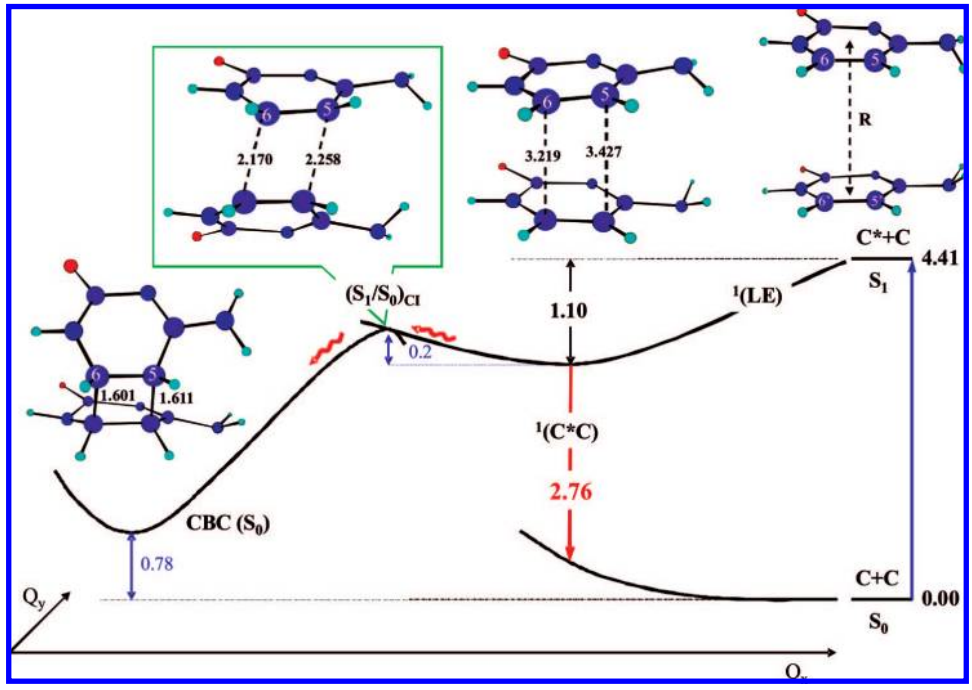

Figure 6. CASPT2 results for the computed decay path of the lowest singlet excited state (S_1) of the cytosine dimer involving the relaxed excimer ^{1}(C*C) through the conical intersection $(S_1/S_0)_{CI}$ leading to ground-state cyclobutane cytosine (CBC). The photoreaction competes with the fluorescence from ^{1}(C*C). The main intermolecular geometric parameters (in Å) are included. The remaining numerical values (in eV) correspond to relative energies, as indicated, with respect to two ground-state cystosine molecules separated $R \cong 10.5$ Å. The Q_x coordinate is mainly related to the average intermolecular distance of $R(C_5-C_{5'})$ and $R(C_6-C_{6'})$, whereas Q_y is associated with the remaining degrees of freedom.

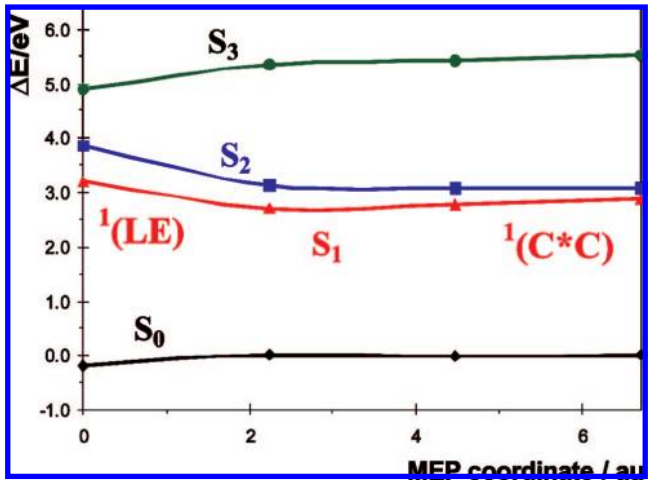

Figure 7. Low-lying singlet excited states of the cytosine dimer computed at the CASPT2//CASSCF level along the minimum energy path (MEP) of the S_1 state from the geometry of the singlet locally excited state ^{1}(LE). The S_1-MEP ends at the relaxed excimer ^{1}(C*C) (see Figure 6).

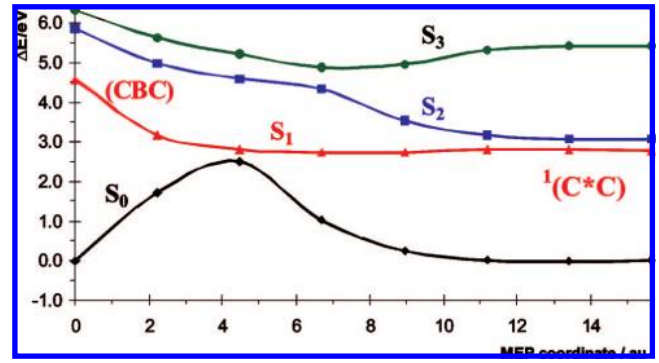

Figure 8. Low-lying singlet excited states of the cytosine dimer computed at the CASPT2//CASSCF level along the minimum energy path (MEP) of the S_1 state from the cyclobutane cytosine (CBC) dimer at its ground-state equilibrium geometry. The S_1-MEP ends at the relaxed excimer ^{1}(C*C) (see Figure 6).

the dramatic wavelength dependence seen by using fluorescence polarization measurements of the pure excimer fluorescence observed for CpC in neutral ethylene glycol/water glasses at low temperatures.[75,76] Thus, when the excitation wavelength (λ_e) used is 250 nm (4.96 eV), the recorded fluorescence wavelength (λ_f) becomes 310 nm (4.00 eV), whereas at $\lambda_e = 300$ nm (4.13 eV) the observed emission is $\lambda_f = 460$ nm (2.70 eV). Even if the results computed in vacuo are not strictly comparable to those data derived from glycol/water glasses, it is tempting to anticipate qualitatively that when λ_e is shorter (case A) or longer (case B) than the absorption maximum (λ_{max}) of the monomer, computed at 4.41 eV, the fluorescence observed for CpC could be related to the ^{1}(LE)-type excimer or to a relaxed ^{1}(C*C)-type excimer, respectively. The predicted fluorescence from the relaxed excimer ^{1}(C*C), 2.76 eV, is indeed consistent with case B (2.70 eV).[75,76] The observed variation in the polarization character could then be attributed basically to the different nature of the systems responsible of the fluorescent features in the unrelaxed (case A) and relaxed (case B) excimers.

The presence of a conical intersection as the main actor in the photoinduced production of bipyrimidine lesions along the singlet manifold is intrinsic to any ethene-like dimer system such as the cytosine dimer. For this reason, examination of the results for the crossing $(S_1/S_0)_{CI}$ in the ethene dimer itself, employing the same tools and computational strategies as described above, is illustrative. Figure 9 shows the $(S_1/S_0)_{CI}$

(75) Callis, P. R. *Chem. Phys. Lett.* **1973**, *19*, 551–555.
(76) Wilson, R. W.; Callis, P. R. *J. Phys. Chem.* **1976**, *80*, 2280–2288.

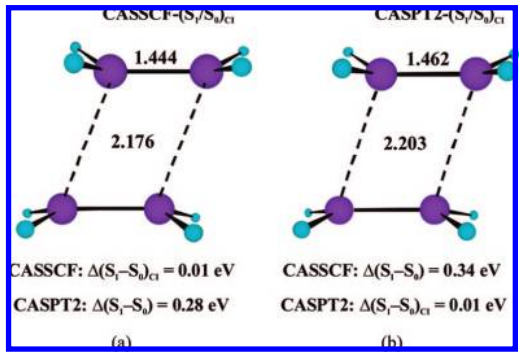

Figure 9. Conical intersection $(S_1/S_0)_{CI}$ of the ethene dimer and energy difference between the implied states at the different levels of theory (a) at the CASSCF(4,4) optimized geometry, and (b) at the CASPT2(4,4) optimized geometry. Distances in Å.

optimized geometry computed at the CASSCF(4,4) and CASPT2(4,4) levels of theory by using analytical and numerical gradients, respectively. The $(S_1/S_0)_{CI}$ structures are of rhomboid type and agree with previous results based on large-scale MRCI and CASPT2 computations.[77,78] As can be readily seen in Figure 9, dynamic electron correlation accounted for at the CASPT2 level tends to increase the intra- and interbond distances. On the other hand, at the optimized geometry for the CASSCF crossing, the energy difference between the two states becomes 0.28 eV at the CASPT2 level, whereas at the conical intersection computed at the CASPT2 level, the CASSCF energy difference is 0.34 eV. A similar situation happens for the cytosine dimer, where the CASSCF and CASPT2 conical intersections are placed in different regions of the hypersurface. The differential electron correlation between S_0 and S_1 at the region of crossing is relevant both qualitatively and quantitatively. While $(S_1/S_0)_{CI}$ is below the relaxed excimer ^{1}(C*C) at the CASSCF level, the former is separated by a barrier height of 0.2 eV from the latter at the CASPT2 level. In other words, the pathway is predicted barrierless by using the CASSCF approach. In contrast the more advanced CASPT2 method offers a completely different picture (cf. Figure 6). The ethenic bond lengths (C_5-C_6) and ($C_{5'}$-$C_{6'}$) at the $(S_1/S_0)_{CI}$ geometry, 1.471 Å and 1.422 Å, respectively, are elongated with respect to the relaxed ^{1}(C*C) excimer, 1.399 Å, and shorter than those in CBC, 1.539 Å. In the meantime, a progressive decrease of the intramonomer bond distances $C_5-C_{5'}$ and $C_6-C_{6'}$ takes place from ^{1}(C*C) to CBC passing through $(S_1/S_0)_{CI}$. These structural changes reflect the conversion process involving the transformation of two carbon−carbon double bonds into single bonds, together with the simultaneous formation of two new single carbon−carbon bonds.

While the photoinduced [2 + 2] cycloaddition of two stacked cytosine molecules proceeds through a stepwise mechanism in the triplet manifold, the photoreaction occurs via a concerted mechanism on the lowest singlet excited state. The former is mediated by a singlet−triplet crossing and the latter takes place through a singlet−singlet conical intersection, which are the funnels for the ultrafast nonradiative decay leading to CBC. The singlet−triplet crossing can be accessed barrierless, but the efficiency of the process relies on the effectiveness of the ISC mechanism. On the other hand, a small barrier (0.2 eV) has to be overcome along the studied pathway in the singlet manifold to reach the conical intersection, but there might be many different orientations in the vicinity of the crossing $(S_1/S_0)_{CI}$ prone to react directly with no barrier. Figure 6 just shows that from the most plausible reactive species, a relaxed excimer characterized by a large binding energy, a small barrier to reach the funnel does exist. Figure 10 displays a scheme of CBC formation through both singlet and triplet manifold. Within the present context, a key question rises: Why is thymine more reactive than cytosine? Because of the methyl group in thymine, the corresponding thymine excimers are expected to be less stable than those of cytosine. In this respect, thymine can be considered more reactive toward the formation of photoinduced dimers than cytosine because the lack of competitive stable thymine excimers. The present picture is supported by independent experimental research. On the one hand, excimer contributions to the total fluorescence yield were found less prominent in $(dT)_{15}$ than in $(dC)_{15}$.[47] On the other hand, the transient absorption signals at 570 nm from $(dT)_{18}$ and its 5′-mononucleotide TMP agree within experimental uncertainty, that is, formation of thymine excimers was not observed.[7] Both facts point out to the absence of thymine excimers. Consequently, the decay of the thymine-base monomer via internal conversion becomes the main deactivation route, whereas for cytosine oligomers it competes with the formation of stable excimers bearing well characterized photophysical properties.[16,47] In addition, as we have shown here, cytosine excimers can also be considered as precursors of mutagenic photoproducts. Thus, when a system is able to form stable singlet excimers placed at energies below the crossing with the ground state, as it is the case of cytosine, formation of photoproducts along the singlet mechanism should proceed at a slower relative rate for these orientations, because of the presence of a barrier to be overcome, making the full process less efficient (see Figure 10). Furthermore, taking into consideration that a very recent study based on femtosecond time-resolved infrared spectroscopy shows that thymine dimers are fully formed around 1 ps after UV excitation,[9] it is tempting to propose that the intrinsic ultrafast photoreactivity of the thymine dimer is partially due to the absence of stable thymine excimers, since, in practice, basically all the relative orientations of the two monomers close to the region where the corresponding conical intersection[11,12] takes place become potentially *reactive.* In accordance with the fact that no stable excimers are formed, the initial *reactive orientations* (shadowed regions in Figure 10) are expected to reach the funnel in a barrierless mode because they are at higher energies than the conical intersection $(S_1/S_0)_{CI}$. Nevertheless, the accessibility of the area around the funnel would be ultimately dictated by the inherent flexibility of the biopolymer under consideration.

Conclusions

The present contribution emphasizes the importance of excimers to understand not only the distinct photophysics of oligonucleotides, as well as DNA itself, but also to rationalize the intrinsic and distinct photoinduced reactivity of cytosine and thymine toward the formation of cyclobutane dimers, recognized as one of the most common processes leading to DNA damage under UV irradiation. Taking as starting structures the locally excited ^{3}(LE) and ^{1}(LE) excimers, which have a face-to-face arrangement at the ground-state geometry of the cytosine monomer, it is shown on the basis of high-level ab initio computations that a stepwise intermediate, ^{3}(SWI), is produced with no barrier in the triplet manifold, whereas the barrierless

(77) Serrano-Andrés, L.; Merchán, M.; Lindh, R. *J. Chem. Phys.* **2005**, *122*, 104107.
(78) Dallos, M.; Lischka, H.; Shepard, R.; Yarkony, D. R.; Szalay, P. G. *J. Chem. Phys.* **2004**, *120*, 7330–7339.

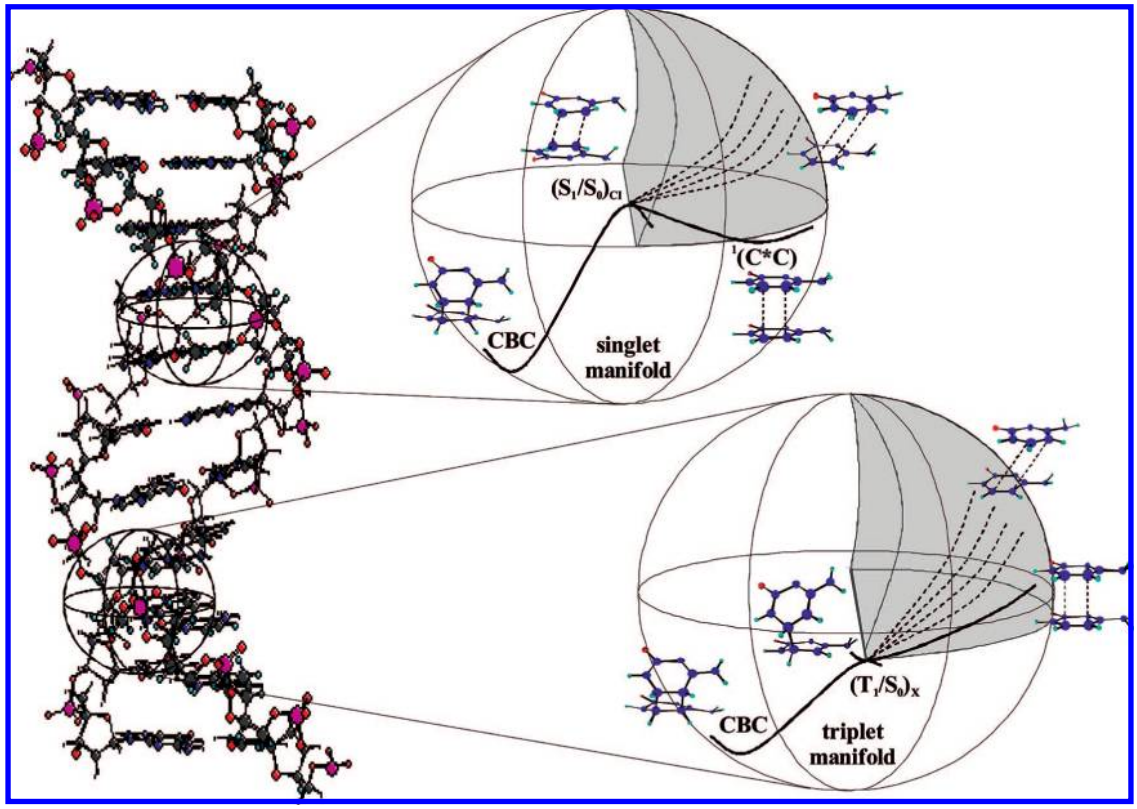

Figure 10. Scheme of the photodimerization process of the π-stacked cytosine dimer along the singlet and the triplet manifold. The shadowed volumes in the sphere represent regions of the DNA strand with reactive orientations, in which the decay path lies above the singlet−triplet crossing $(T_1/S_0)_X$ and the conical intersection $(S_1/S_0)_{CI}$.

pathway along the lowest singlet hypersurface yields the relaxed excimer ^{1}(C*C). The structure ^{3}(SWI) has a covalent single bond between the carbon atoms $C_6-C_{6'}$, with the $C_5-C_{5'}$ bond length kept long. The required energy to reach ^{3}(SWI) from two isolated ground-state cytosine monomers, 2.70 eV, is related to the threshold observed experimentally for a given photosensitizer to become a potential DNA photodamager, and it is in agreement with the triplet energy of thymine in DNA deduced experimentally, 2.80 eV.[50] At the ^{3}(SWI) structure a singlet−triplet crossing $(T_1/S_0)_X$ takes place, which mediates the nonradiative deactivation toward the ground state by an intersystem crossing mechanism (ISC). Under favorable conditions for spin−orbit coupling (SOC) and according to the barrierless profile computed, the decay is predicted to take place on a subpicosecond range. Because the ^{3}(SWI) intermediate is obtained from many different initial structures (see Figure 10), the findings can also be applied in situations where no excimers are expected to be present. Thus, the results offer a nice rationale to the known fact that pyrimidine dimers are formed in solution under triplet photosensitization conditions[1] and the lack of any triplet absorption in the transient spectra reported for $(dT)_{20}$ due to the high efficiency of the process compared to the time resolution used to monitor the thymine dimer formation.[8]

The *shearing-type* conical intersection involving the lowest singlet and the ground state becomes the cornerstone to understand the formation of photoproducts along the singlet manifold. In order to reach the funnel, the system placed at ^{1}(C*C) has to overcome a barrier of 0.2 eV. In competition to the photoreaction, fluorescence from the ^{1}(C*C) becomes also possible. The fluorescent features from the locally excited ^{1}(LE) and the relaxed ^{1}(C*C) excimers help to rationalize the pronounced wavelength dependence observed in solution by using fluorescence polarization techniques.[75,76] The presence of a barrier does not imply however that the overall process of formation of cyclobutane cytosine (CBC) is hindered. Instead, analysis of the current theoretical and experimental information at hand suggests as *reactive orientations* those that at the time of light irradiation are close but energetically above the shearing-type conical intersection $(S_1/S_0)_{CI}$, which is concomitant to Pyr<>Pyr formation (see Figure 10). In this sense, the lack of stable excimers represents a larger potential of the system to achieve reactive arrangements, which is translated into a relative higher rate. Such a situation is accomplished by thymine.[7,47] On the contrary, as it occurs in cytosine, stable excimers may decrease the effectiveness of photoproduct formation in the singlet manifold, since the orientations of the monomers around the region of the relaxed excimer might not be so reactive and an excess of vibrational energy is required to surmount the corresponding barriers and, as a result, the CBC formation becomes globally less effective (see Figure 10). In summary, stable singlet excimers slow down the efficiency of dimer formation, as for cytosine, whereas the absence of excimers, such as thymine, may indirectly favor the photoreaction. The scheme serves to rationalize the reason why a reaction which proceeds via triplet state in solution may have a singlet-state precursor when the biochromophores are held together, as is the case in frozen solutions or in a biopolymer.[15] It may also be useful to design health care phototherapeutic nucleobase-based drugs addressed to either enhance or decrease pyrimidine dimer formation by using, for instance, appropriate nucleobases derivatives. Not surprisingly, bioexcimers are ubiquitously used by Nature. They play a fundamental role in photobiology by modulating the

charge redistribution in the lowest excited state, something which is crucial to understand electron transfer in photosynthesis[79] and, as shown here, to rationalize the distinct intrinsic reactivity of DNA nucleobases toward intrastrand pyrimidine dimerization.

Acknowledgment. The research reported has been supported by the MEC-FEDER projects CTQ2007-61260 and CSD2007-0010 Consolider-Ingenio in Molecular Nanoscience. D.R.S., G.O.G., and I.G.R. gratefully acknowledge Ph.D. fellowships from the Spanish MEC.

Supporting Information Available: Further computational details and wave function descriptions, complete ref 56, Cartesian coordinates for the optimized structures, and plots on BSSE-uncorrected curves (PDF). This material is available free of charge via the Internet at http://pubs.acs.org.

JA803068N

(79) Olaso-González, G.; Merchán, M.; Serrano-Andrés, L. *J. Phys. Chem. B* **2006**, *110*, 24734–24739.